

# Structural Fixation of Spontaneous Vesicles in Aqueous Mixtures of Polymerizable Anionic and Cationic Surfactants

Shiyong Liu, Yamaira I. González, and Eric W. Kaler\*

Center for Molecular and Engineering Thermodynamics, Department of Chemical Engineering, University of Delaware, Newark, Delaware 19716

Received August 1, 2003. In Final Form: September 29, 2003

Two polymerizable surfactants, cationic methacryloyloxyundecyl trimethylammonium bromide and anionic sodium 4-(*ω*-methacryloyloxyundecyl)oxy benzene sulfonate, have been synthesized. The microstructures formed by mixtures of these surfactants in aqueous solution include stable vesicles, the structure of which can be fixed by polymerization. Both native and polymerized vesicles are characterized using quasi-elastic and static light scattering, small-angle neutron scattering, and cryogenic transmission electron microscopy. Polymerization captures the bilayer structure without creating appreciable intervesicle cross-linking.

## Introduction

The formation of vesicles or liposomes is a familiar property of bilayer-forming surfactants, such as the phospholipids that constitute the major component of cell walls.<sup>1</sup> These hollow spherical structures are composed of an amphiphilic bilayer that encloses an aqueous interior volume. Vesicles are useful as biological membrane models, drug delivery vehicles, or nanocompartments for the formation of biomaterials.<sup>2–5</sup> An approach to forming unilamellar vesicles is provided by the mixing of cationic and anionic surfactants,<sup>6–16</sup> and the thermodynamics of the formation of these structures has received detailed attention.<sup>17–19</sup> In many of these mixtures, vesicles form

spontaneously and the vesicles are infinitely stable if solution conditions (concentration, pH, ionic strength, etc.) are kept unchanged.

Alternatively, vesicles can also be formed far from thermodynamic equilibrium through sonication or mechanical disruption of bilayer phases, techniques which do not allow close control of the vesicle size and structure.<sup>20,21</sup> These metastable vesicles, which are typically formed by the dispersion of bilayer phases of double-chained surfactants, will ultimately revert to stable flat bilayer structures with a resulting loss of integrity, limiting their use in many applications. As a result, one route to structural stabilization is the polymerization of vesicles, a process that locks into place the nonequilibrium vesicle structures.<sup>7,22–28</sup> In most cases, this has required the synthesis of phospholipid analogues incorporating a polymerizable group (e.g., a vinyl moiety). An alternate route to structural stabilization is polymerization *in* vesicles, in which case kinetically stabilized vesicles are used as templates for the synthesis of stabilized hollow nanostructures. In this approach, hydrophobic monomers swell the vesicle bilayers and are subsequently polymerized.<sup>29–32</sup> Detailed studies suggest that in most cases polymerization yields solid latex polymer particles at

\* To whom correspondence should be addressed. E-mail: kaler@che.udel.edu. Tel: (302)831-3553. Fax: (302)831-6751.

(1) New, R. R. C. In *Liposomes: A Practical Approach*, New, R. R. C., Ed.; IRL Press: Oxford, 1990; p 33–103.

(2) Philippot, J. R.; Schuber, F. In *Liposomes as Tools in Basic Research and Industry*; Philippot, J. R., Schuber, F., Eds.; CRC Press: Boca Raton, FL, 1994; p 276.

(3) Tanev, P. T.; Pinnavaria, T. J. *Science* **1996**, *271*, 1267–1269.

(4) Lasic, D. D.; Papahadjopoulos, D. *Science* **1995**, *267*, 1275–1276.

(5) Kunitake, T. *Angew. Chem., Int. Ed. Engl.* **1992**, *31*, 709–726.

(6) Kaler, E. W.; Murthy, A. K.; Rodriguez, B. E.; Zasadzinski, J. A. N. *Science* **1989**, *245*, 1371–1374.

(7) Brasher, L. L.; Kaler, E. W. *Langmuir* **1996**, *12*, 6270–6276.

(8) Iampietro, D. J.; Kaler, E. W. *Langmuir* **1999**, *15*, 8590–9601.

(9) Talhout, R.; Engberts, B. F. N. *Langmuir* **1997**, *13*, 5001–5006.

(10) Sakai, H.; Matsumura, A.; Yokoyama, S.; Saji, T.; Abe, M. *J. Phys. Chem. B* **1999**, *103*, 10737–10740.

(11) Söderman, O.; Herrington, K. L.; Kaler, E. W.; Miller, D. D. *Langmuir* **1997**, *13*, 5531–5538.

(12) Marques, E.; Khan, A.; Miguel, M. D.; Lindman, B. *J. Phys. Chem.* **1993**, *97*, 4729–4736.

(13) Yacilla, M. T.; Herrington, K. L.; Brasher, L. L.; Kaler, E. W.; Chiruvolu, S.; Zasadzinski, J. A. N. *J. Phys. Chem.* **1996**, *100*, 5874–5879.

(14) Fischer, A.; Hebrant, M.; Tondre, C. *J. Colloid Interface Sci.* **2002**, *248*, 163–168.

(15) Mao, M.; Huang, J.; Zhu, B.; Yin, H.; Fu, H. *Langmuir* **2002**, *18*, 3380–3382.

(16) Walker, S. A.; Zasadzinski, J. A. *Langmuir* **1997**, *13*, 5076–5081.

(17) Laughlin, R. G. *Colloids Surf., A* **1997**, *128*, 27–38.

(18) (a) Horbaschek, K.; Hoffmann, H.; Hao, J. C. *J. Phys. Chem. B* **2000**, *104*, 2781–2784. (b) Hao, J. C.; Hoffmann, H.; Horbaschek, K. *J. Phys. Chem. B* **2000**, *104*, 10144–10153.

(19) Jung, H. T.; Lee, S. Y.; Kaler, E. W.; Coldren, B.; Zasadzinski, J. A. *Proc. Natl. Acad. Sci. U.S.A.* **2002**, *99*, 15318–15322. (b) Jung, H. T.; Coldren, B.; Zasadzinski, J. A.; Iampietro, D. J.; Kaler, E. W. *Proc. Natl. Acad. Sci. U.S.A.* **2001**, *98*, 1353–1357.

(20) Hauser, H.; Mantsch, H. H.; Casal, H. L. *Biochemistry* **1990**, *29*, 2321–2329.

(21) Liu, S.; O'Brien, D. F. *J. Am. Chem. Soc.* **2002**, *124*, 6037–6042.

(22) (a) Hirano, K.; Fukuda, H. *Langmuir* **1991**, *7*, 1045–1047. (b) Chung, M.-H.; Chung, Y.-C. *Colloids Surf., B* **2002**, *24*, 111–121.

(23) Tondre, C.; Caillet, C. *Adv. Colloid Interface Sci.* **2001**, *93*, 115–134.

(24) (a) Sisson, T. M.; Lamparski, H.; Kölchens, S.; Elyadi, A.; O'Brien, D. F. *Macromolecules* **1996**, *29*, 8321–8329. (b) Regen, S. L.; Singh, A.; Oehme, G.; Singh, M. *J. Am. Chem. Soc.* **1982**, *104*, 791–795.

(25) Liu, S.; Sisson, T. M.; O'Brien, D. F. *Macromolecules* **2001**, *34*, 465–473.

(26) Peek, B. M.; Callahan, J. H.; Namboodiri, K.; Singh, A.; Gaber, B. P. *Macromolecules* **1994**, *27*, 292–297.

(27) Abid, S. K.; Sherrington, D. C. *Polymer* **1992**, *33*, 175–180.

(28) Jung, M.; den Ouden, I.; Montoya-Goñi, A.; Hubert, D. H. W.; Frederik, P. M.; van Herck, A. M.; German, A. L. *Langmuir* **2000**, *16*, 4185–4195.

(29) Kurja, J.; Nolte, R. J. M.; Maxwell, I. A.; German, A. L. *Polymer* **1993**, *34*, 2045.

(30) Hotz, J.; Meier, W. *Langmuir* **1998**, *14*, 1031–1036.

(31) Murthagh, J.; Thomas, J. K. *Faraday Discuss. Chem. Soc.* **1986**, *81*, 127–136.

(32) Poulain, N.; Nakache, E.; Pina, A.; Levesque, G. *J. Polym. Sci., Part A: Polym. Chem.* **1996**, *34*, 729–737.

tached to the original vesicle structure rather than the desired hollow polymer vesicles.<sup>33,34</sup>

In contrast, monomer can also be taken up into the hydrophobic bilayer of spontaneous unilamellar vesicles. Subsequent polymerization and dialysis yield hollow spheres composed of polymer made from the incorporated hydrophobic monomers.<sup>35–37</sup> Despite this success, there are several issues with this approach. First, upon the addition of a hydrophobic monomer, the structure of the initial stable vesicles can change or evolve to other microstructures;<sup>17</sup> second, the surfactant providing the vesicle template needs to be removed (usually by dialysis, which is time-consuming) before the hollow nanospheres can be isolated; and finally, the hollow nanospheres, which are hydrophobic, can only be redispersed in water with the aid of a surfactant or after chemical modification.

To avoid these complications, it would be useful to produce hydrophilic (charged) hollow polymer spheres directly from vesicles. The use of spontaneous unilamellar vesicles also offers the possibility of exploiting equilibrium self-assembly principles to accurately control the vesicle size and bilayer thickness. The method requires only the preparation of mixed solutions of polymerizable surfactants and subsequent facile polymerization. To develop this approach, two polymerizable surfactants, methacryloyloxyundecyl trimethylammonium bromide (MUTB) and sodium 4-( $\omega$ -methacryloyloxyundecyl)oxy benzene sulfonate (MUBS), were synthesized. Spontaneous and stable vesicles were formed from the combination of micellar solutions of MUTB and MUBS. These vesicles were then polymerized to fix the vesicular structure. Both the original and polymerized vesicles were characterized using quasi-elastic and static light scattering (QLS, SLS), small-angle neutron scattering (SANS), and cryogenic transmission electron microscopy (cryo-TEM). The unilamellar vesicle structure has been successfully fixed by polymerization. Although the polymerization of vesicles formed from phospholipids with double bonds has been reported some time ago,<sup>22–28</sup> this is the first report of direct structural fixation of spontaneous and stable vesicles without the addition of other components. Previous experiments with ion-paired amphiphiles (IPAs)<sup>22</sup> relied on sonication to form vesicles, and there are considerable differences between IPAs and the more general anionic/cationic surfactants considered here.<sup>23</sup>

## Materials and Methods

**Materials.** Methacryloyl chloride was distilled under reduced pressure and stored at 4 °C. 11-Bromoundecanol, phenol-4-sulfonic acid sodium salt dehydrate, KOH, trimethylamine (anhydrous), anhydrous tetrahydrofuran (THF), and ethyl ether were purchased from Aldrich. Dowex 50W-X8(H) ion-exchange resin was obtained from BDH. The initiator, 2,2'-azobis(2-amidinopropane) hydrochloride (V50) (Wako Pure Chemical Industries, Ltd.), was recrystallized from methanol.

**Preparation of MUTB.** 11-Bromoundecyl Methacrylate. 11-Bromoundecanol (20 g, 0.08 mol) and 320 mL of anhydrous THF were mixed in a flask at 0 °C under N<sub>2</sub>, followed by the addition

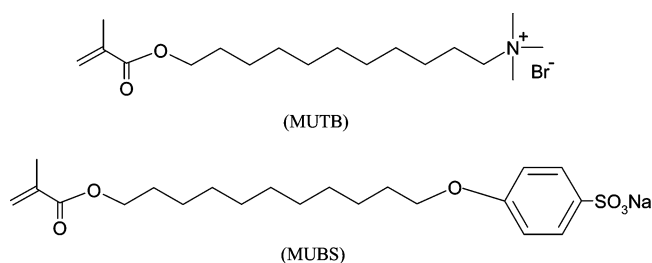


**Figure 1.** Chemical structures of the cationic surfactant methacryloyloxyundecyl trimethylammonium bromide (MUTB) and the anionic surfactant sodium 4-( $\omega$ -methacryloyloxyundecyl)oxy benzene sulfonate (MUBS).

of 10.8 mL (0.11 mol) of methacryloyl chloride. The reaction system was bubbled with N<sub>2</sub> at room temperature for 2 h and then left stirring overnight. The unreacted methacryloyl chloride and solvent were removed under reduced pressure. The yellowish residue was dissolved in ethyl ether and washed with saturated sodium hydrogen carbonate solution until the aqueous layer was basic. After evaporation of the ether, a viscous yellowish liquid of 11-bromoundecyl methacrylate was obtained with a yield of 91%.<sup>38</sup>

**MUTB.** MUTB (yield, 75%) was conveniently obtained by reacting 11-bromoundecyl methacrylate with trimethylamine gas in diethyl ether at 0 °C as described by Michas et al.<sup>39</sup>

**Preparation of MUBS.** 4-(11-Hydroxyundecyl)oxy Benzene Sulfonic Acid (HBSA-11). Phenol-4-sulfonic acid sodium dihydrate (29.26 g, 0.126 mol), KOH (7.07 g, 0.126 mol), and 120 mL of H<sub>2</sub>O were mixed in a 500 mL round-bottom flask equipped with a condenser. 11-Bromoundecanol (30.15 g, 0.12 mol) in 180 mL of ethanol was added, and the reaction mixture was refluxed overnight. A white precipitate of 4-(11-hydroxyundecyl)oxy benzene sulfonate formed when the reaction mixture was cooled in an ice-water bath. The solid was filtered and washed with chloroform to remove 11-bromoundecanol and purified by recrystallization from hot water. The white product obtained was dissolved in hot distilled water and eluted through a Dowex 50W-X8(H) ion exchange column preheated to 60–70 °C. After this elution process, 4-(11-hydroxyundecyl)oxy benzene sulfonate was converted to its sulfonic acid form. The effluent was freeze-dried to yield a white, fluffy solid.<sup>40</sup>

**MUBS.** In a 500 mL, three-neck, round-bottom flask equipped with an air-leak and dropping funnel, 4-(11-hydroxyundecyl)oxy benzene sulfonic acid (20 g, 0.061 mol) was dissolved in 200 mL of dry THF. Methacryloyl chloride (15.14 mL, 0.155 mol) and 0.14 g (0.0012 mol) of hydroquinone in 30 mL of dry THF were added dropwise. The reaction mixture was stirred for 48 h under N<sub>2</sub> protection. Unreacted methacryloyl chloride and THF were removed in vacuo. Ether was added to the orange brown oil residue, and then a saturated brine solution was added to convert the sulfonic acid into its sodium salt form. MUBS was washed with ether and dried before it was recrystallized from methanol. Purified MUBS was obtained as a white powder, and the overall yield was 70%.<sup>40</sup>

The chemical structures of MUTB and MUBS are shown in Figure 1 and were verified by <sup>1</sup>H NMR.

**Preparation of Vesicles, Phase Diagram Determination, and Polymerization.** Samples were prepared by first making stock solutions of MUTB and MUBS at the desired concentration and temperature in deionized water. Since the anionic surfactant MUBS has a Krafft point of 43 °C, all the stock solutions were kept at 50 °C before mixing. Vesicle samples were prepared by vortex-mixing the stock solutions for 10 s at the desired ratio and then holding the samples in a water bath thermostated at 25 °C.

For samples prepared for phase diagram measurement, several crystals of hydroquinone were added to the mixed solution to prevent any polymerization. Samples were thermostated at 25

(33) (a) Hentze, H. P.; Kaler, E. W. *Curr. Opin. Colloid Interface Sci.* **2003**, *8*, 164–178. (b) Hentze, H. P.; Co, C. C.; McKelvey, C. A.; Kaler, E. W. *Top. Curr. Chem.* **2003**, *226*, 197–223.

(34) (a) Jung, M.; Hubert, D. H. W.; Bomans, P. H. H.; Frederik, P. M.; Meuldijk, J.; van Herk, A. M.; Fischer, H.; German, A. L. *Langmuir* **1997**, *13*, 6877–6880. (b) Jung, M.; Hubert, D. H. W.; Bomans, P. H. H.; Frederik, P. M.; van Herk, A. M.; German, A. L. *Adv. Mater.* **2000**, *12*, 210–213.

(35) Morgan, J. D.; Johnson, C. A.; Kaler, E. W. *Langmuir* **1997**, *13*, 6447–6451.

(36) McKelvey, C. A.; Kaler, E. W.; Zasadzinski, J. A.; Coldren, B.; Jung, H.-T. *Langmuir* **2000**, *16*, 8285–8290.

(37) McKelvey, C. A.; Kaler, E. W. *J. Colloid Interface Sci.* **1996**, *179*, 587.

(38) Hamid, S. M.; Sherrington, D. C. *Polymer* **1987**, *28*, 325–331.

(39) Michas, J.; Paleos, C. M.; Dais, P. *Liq. Cryst.* **1989**, *5*, 1737–1745.

(40) Xu, X. J.; Goh, H. L.; Siow, K. S.; Gan, L. M. *Langmuir* **2001**, *17*, 6077–6085.

°C for at least 3 days. Phases were examined by eye to determine the number of phases. Single phases displaying Tyndall scattering were identified as possible vesicle phases, with the presence or absence of vesicle structures ultimately determined by the methods described below.

For the polymerization of vesicle samples, aqueous mixtures of two surfactants with molar ratios of [MUTB]/[MUBS] = 7:3 or [MUTB]/[MUBS] = 4:6 and a total concentration of 27 mM were prepared (27 mM MUTB is equal to 1.02 wt %, while 27 mM MUBS is equal to 1.17 wt %). The water-soluble initiator V50 was added (the molar ratio of ([MUTB + MUBS])/[V50] was fixed at 70/1), and the polymerization was carried out at 58 °C.

**QLS and SLS.** QLS and SLS measurements were made using equipment manufactured by Brookhaven Instruments Corp. (BI9000). The scattering angle was fixed at 90°. Samples thermostated at 25 °C were irradiated with 488 nm light produced from a Loxel 2 W argon ion laser. Intensity correlation data were analyzed by the method of cumulants to provide the average decay rate,  $\langle \Gamma \rangle (=q^2 D)$ , where  $D$  is the diffusion coefficient, and the normalized variance,  $\nu (=([\Gamma^2] - \langle \Gamma \rangle^2)/\langle \Gamma \rangle^2)$ , which is a measure of the width of the distribution of the decay rates.<sup>41</sup> The measured diffusion coefficients were represented in terms of apparent radii by using Stokes law and assuming the solvent had the viscosity of water. Stock solutions of each pure surfactant were filtered through 0.22  $\mu\text{m}$  Millipore Acrodisc-12 filters prior to preparing samples.

In SLS, the angular dependence of the excess absolute time-averaged scattered light intensity, known as the Rayleigh ratio  $R_w(q)$ , of a series of diluted polymerized vesicle solutions (concentrations ranging from  $6.490 \times 10^{-5}$  to  $2.531 \times 10^{-4}$  g/mL) led to the apparent weight-average molar mass ( $M_w$ )<sub>app</sub> and the root-mean-square  $z$ -average radius of gyration ( $R_g$ ) <sub>$z$</sub> <sup>1/2</sup> (written as  $\langle R_g \rangle$ ).  $q$  is the scattering vector. The  $dn/dc$  value (0.12 mL/g) of polymerized vesicle solutions ([MUTB]/[MUBS] = 7:3) was measured at 25 °C using an interferometric refractometer ( $\lambda = 488$  nm) for a range of concentrations.

**SANS.** SANS measurements were made at the National Institute of Standards and Technology (NIST) in Gaithersburg, MD. An average radiation wavelength of 6 Å with a spread of 11% was used. Samples were held at 25 °C in quartz “banjo” cells with 1 mm path lengths. Three sample–detector distances were used to give a range in scattering vector of 0.005–0.5 Å<sup>-1</sup>. The data were corrected for detector efficiency, background, and empty cell scattering and placed on an absolute scale using NIST procedures.

**SANS Modeling.** A polydisperse core–shell model was used to fit the SANS spectra measured for both the original vesicles and polymerized vesicles. The vesicles were assumed to have a polydisperse core with constant shell thickness. Polydispersity was described by a Schulz distribution.<sup>42</sup> The adjustable parameters for this model were the (polymerized) vesicle core diameter, shell thickness, and polydispersity. These parameters were varied to minimize the value of  $\chi^2$  for the model fit to each SANS spectrum. The volume fraction of the scatterers was calculated from a mass balance assuming that all the surfactant had formed vesicles and that no free surfactant was present in the aqueous solution. The scattering length densities (SLDs) for each component were calculated by summing the scattering amplitudes of each group or atom in a molecule and dividing this total by the sum of the respective volumes. For MUTB and MUBS, the calculated SLDs are  $2.1 \times 10^{-7}$  and  $9.9 \times 10^{-7}$  Å<sup>-2</sup>, respectively. The scattering length density of D<sub>2</sub>O is  $6.3 \times 10^{-6}$  Å<sup>-2</sup>.

**Cryo-TEM.** Specimens for cryo-TEM were prepared in a controlled environment vitrification system (CEVS) described in detail by Bellare et al.<sup>43</sup> The sample vial was opened to withdraw the sample after the chamber contents were equilibrated at the desired temperature (25 °C) and relative humidity (95–99%). Specimens of the microstructured liquid were prepared by placing a drop of the sample on a lacey carbon film, supported by a copper grid (Ted Pella, Redding, CA) held by a pair of self-

**Table 1. Krafft Temperature ( $T_k$ ) of Mixed MUTB and MUBS Surfactant Solutions at Various Molar Ratios and a Total Surfactant Concentration of 27 mM**

	MUTB/MUBS molar ratio							
	9:1	7:3	6:4	4:6	3:7	2:8	1:9	0:10
overall Krafft temp (°C)	<5	16	18	20	24	31	37	43

locking tweezers mounted on a spring-loaded shaft inside the environmental chamber. Thin liquid films of 50–500 nm cross sections were then formed by gently blotting away excess liquid on the grid by touching it with a filter paper. The liquid films were then vitrified by plunging the grid into liquid ethane, held at –180 °C by a surrounding thermostated pool of liquid nitrogen. The grid was then transferred under liquid nitrogen onto the tip of a Gatan model 626 cold stage. Specimens were held at below –168 °C and imaged at 100 kV in a transmission electron microscope (model 2000 FX JEOL). Images were recorded using a Multiscan Gatan CCD camera at low dose.

**Surface Tension.** Surface tension measurements were made using a K10T digital tensiometer (Krüss) with a Wilhelmy plate. All surface tension glassware was acid-washed prior to use. Samples were maintained at 25 °C for MUTB and 50 °C for MUBS by thermostated circulating water.

**NMR Spectroscopy.** NMR measurements were performed at 25 °C on a Bruker AC250 NMR spectrometer (resonance frequency of 250 MHz for <sup>1</sup>H) operating in the Fourier transform mode.

## Results and Discussion

**Surface Properties of MUTB and MUBS.** MUTB has a Krafft point below 5 °C. Surface tension measurements indicate that the critical micelle concentration (cmc) of pure MUTB surfactant monomer is 15 mM at 25 °C, which is consistent with values reported in the literature.<sup>38,44</sup> MUBS, in contrast, has a Krafft point of 43 °C and therefore is not soluble in water at room temperature, although surfactants with similar structure but shorter tail groups are readily soluble at room temperature and have Krafft points less than 20 °C.<sup>40</sup> The cmc of MUBS determined from surface tension measurements is 1.8 mM at 50 °C. Table 1 shows the Krafft temperature ( $T_k$ ) of mixed surfactant solutions at various mixing ratios. As expected, the overall Krafft point decreases monotonically with increasing molar fraction of the low Krafft point MUTB surfactant. The systematic change of the  $T_k$  with the mixing ratios strongly suggests the formed vesicles or other microstructures are still fluid above  $T_k$ .

**Phase Behavior.** A partial phase map for mixtures of MUTB/MUBS/H<sub>2</sub>O at 25 °C in the water-rich corner (<50 mM, about 2 wt %) is shown in Figure 2. Note that the phase rule does not allow a rigorous representation of a mixture of two salts and water at constant temperature on a triangular diagram. Since stable catanionic vesicles of MUTB and MUBS could be obtained at 25 °C (QLS reveals that the size of the catanionic vesicles does not change over the temperature range of 20–50 °C), this temperature was chosen for characterization convenience although it is below  $T_k$  in part of the MUBS-rich region. Samples close to equimolar ratio contain a vesicle phase in equilibrium with precipitate. On the MUTB-rich side, micelles form up to a mixing molar ratio of about  $R = 0.16$  ( $R = [\text{MUBS}]/([\text{MUBS}] + [\text{MUTB}])$ ). QLS measurements of samples with  $R < 0.16$  reveal intensity-averaged hydrodynamic diameters,  $\langle D_h \rangle$ , of 4–15 nm. These dimensions and the fact that the solutions are clear suggest the presence of micellar structures. When additional MUBS is added, a bluish solution, which is a signature for the presence of vesicles, is observed. For mixtures with a total

(41) Koppel, D. E. *J. Chem. Phys.* **1972**, *57*, 4814–4820.

(42) Bartlett, P.; Ottewill, R. H. *J. Chem. Phys.* **1992**, *96*, 3306–3318.

(43) Bellare, J. R.; Davis, H. T.; Scriven, L. E.; Talmon, Y. *J. Electron Microsc. Tech.* **1988**, *10*, 87–111.

(44) Hamid, S. M.; Sherrington, D. C. *Br. Polym. J.* **1984**, *16*, 39–45.

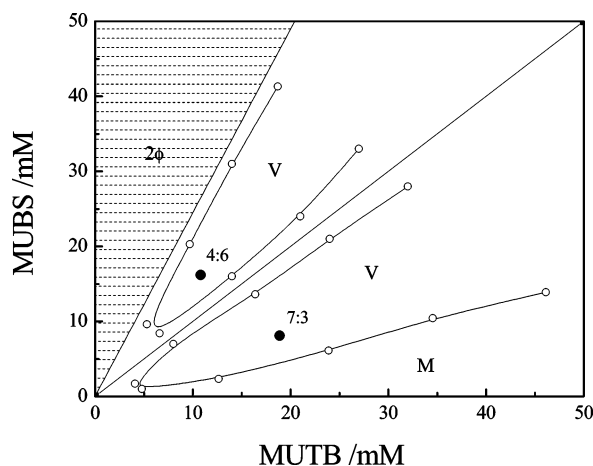


**Figure 2.** Partial phase map at 25 °C for mixtures of cationic surfactant MUTB and anionic surfactant MUBS. The phase regions are micelles (M), vesicles (V), and a two-phase region consisting of precipitate and an isotropic liquid phase (2 $\phi$ ). The ● symbols mark the compositions polymerized.

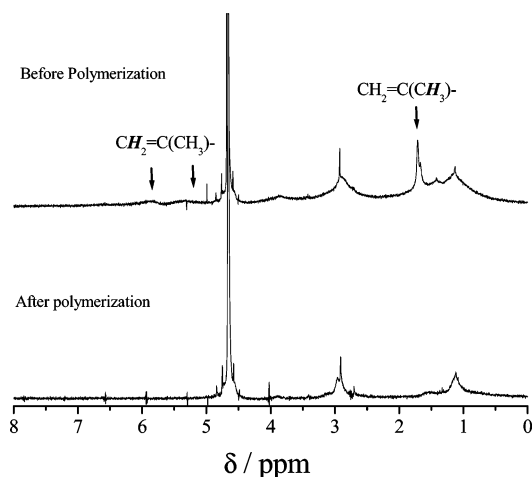


**Figure 3.**  $^1\text{H}$  NMR spectra of original unpolymerized vesicles and polymerized vesicles at 25 °C. The molar ratio of MUTB to MUBS is 7:3 with a total concentration of 27 mM.

concentration below 5 mM, further addition of MUBS results in the formation of two phases because the MUBS component crystallizes. Apparently, below this concentration, which is much below the cmc of the low Krafft point MUTB surfactant, MUTB cannot adequately solubilize the MUBS. At the MUBS-rich corner, the vesicle lobe is smaller than that on the MUTB-rich side. For compositions in the upper left diagram, MUBS always crystallizes and this precipitate coexists with an isotropic liquid phase.

**Polymerization.** Two aqueous mixtures with different surfactant molar ratios ( $[\text{MUTB}]/[\text{MUBS}] = 7:3$ , positively charged;  $[\text{MUTB}]/[\text{MUBS}] = 4:6$ , negatively charged) at a total concentration of 27 mM were polymerized with the addition of the water-soluble initiator V50 (compositions shown by ● in Figure 2). Polymerization was conducted at 58 °C for 2 h. The bluish color characteristic of the vesicle phases is unchanged by polymerization. After polymerization of both samples, the resulting structures are stable, with no indication of phase separation or coagulation. Figure 3 shows the  $^1\text{H}$  NMR spectra of vesicles before and after polymerization. For vesicles before polymerization, the signals at  $\delta$  1.7 ( $\text{CH}_3$  on the methacrylate group of both surfactant monomers) and  $\delta$  5.2–5.9 ( $\text{CH}_2$  on the double bond) can be seen clearly. Note that the signal intensities are weakened and broadened because the methacrylate groups are buried inside the

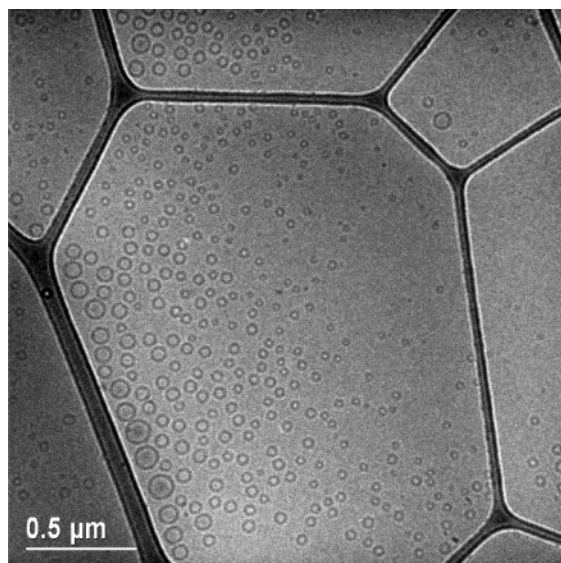


**Figure 4.** Cryo-TEM image of original unpolymerized vesicles (the molar ratio of MUTB to MUBS is 7:3 with a total concentration of 27 mM) showing unilamellar vesicles, whose sizes range from 30 to 100 nm.

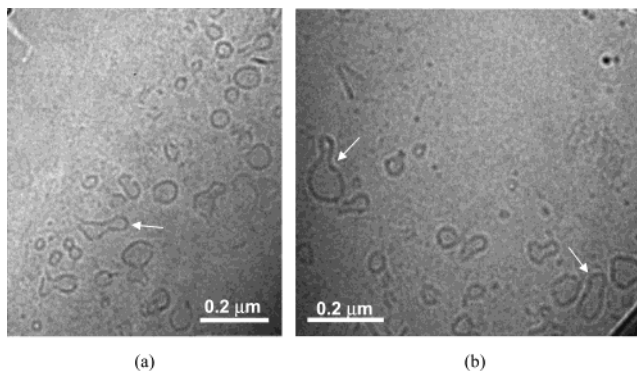


**Figure 5.** Cryo-TEM image of polymerized vesicles (the molar ratio of MUTB to MUBS is 7:3 with a total concentration of 27 mM) showing mostly spherical unilamellar vesicles. Note the presence of a few irregularly shaped vesicles due to vesicle fusion during the polymerization process.

hydrophobic core in the bilayers. After polymerization for 2 h, all the signals characteristic of the unsaturated double bonds have disappeared, indicating complete polymerization of all the double bonds on the surfactant monomers. The polymerized vesicle solutions are stable for over 4 months. Although the freeze-dried samples can be redispersed in water, they could not be molecularly dissolved in any common solvent. Therefore, the degree of polymerization could not be determined.

**TEM Results.** A cryo-TEM micrograph (Figure 4) of the original vesicles shows a distribution of spherical, unilamellar vesicles, whose sizes range from 30 to 100 nm, with the larger vesicles having a characteristic size in agreement with QLS and SANS results (see below). Figure 5 shows cryo-TEM micrographs of the polymerized vesicles at a higher magnification. Unilamellar vesicles are observed, but in these micrographs there is also a mixed population of spherical and irregularly shaped vesicles. The sizes of the polymerized vesicles are comparable to those of the vesicles before polymerization. The irregular unilamellar vesicles are probably the consequence of polymerization, which makes the vesicular shells stiffer. A more complex morphology that appears to be of fused vesicles is highlighted by the arrows. As shown by

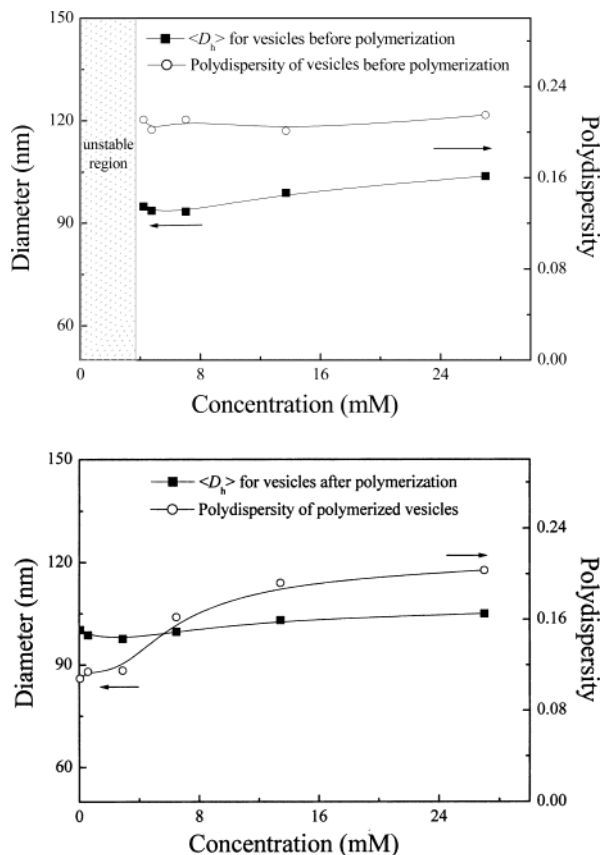


**Figure 6.** The variation of size and polydispersity of unpolymersed vesicles and polymerized vesicles upon dilution. The molar ratio of MUTB to MUBS is 7:3 with a total concentration of 27 mM.

Hubert et al.,<sup>45</sup> such structural transformations could be the result of vesicle fusion caused by the ionic initiator. Water-soluble initiators have also been found to act as hydrotropic salts capable of altering the self-assembly state of surfactant solutions.<sup>46</sup> Nonetheless, the scattering results (see below) are consistent with the predominant polymerization product being vesicles.

**QLS and SLS Results.** Figure 6 shows the variation of the intensity-averaged hydrodynamic diameter ( $D_h$ ) of the original and polymerized vesicles ([MUTB]/[MUBS] = 7:3, total concentration 27 mM) upon dilution. For vesicles before polymerization, QLS reveals an apparent hydrodynamic diameter of about 98 nm, which decreases slightly upon dilution to 5 mM. When the total concentration is below 5 mM, MUBS crystallizes and the sample contains two phases. After polymerization, the size of the vesicles is essentially the same size as before polymerization, that is, 100 nm. Further, the vesicle size does not change upon dilution (up to 400 times; from 27 to 0.07 mM), indicating successful fixation of the vesicular structure. It is interesting to note that the polydispersity of the polymerized vesicles decreases to less than 0.1 upon dilution. This likely reflects the effect of concentration on the QLS measurements. The volume fraction of the vesicles at higher concentrations is ca. 2–3%, so intervesicle interactions could affect the accurate measurement of the vesicle size and polydispersity by QLS. The polymerized vesicle diameter (100 nm) and polydispersity data obtained after high dilution should be considered the true values.

(45) Hubert, D. H. W.; Jung, M.; Frederik, P. M.; Bomans, P. H. H.; Meuldijk, J.; German, A. L. *Langmuir* **2000**, *16*, 8973–8979.

(46) González, Y. I.; Danino, D.; Kaler, E. W. In preparation; to be submitted to *Langmuir*.

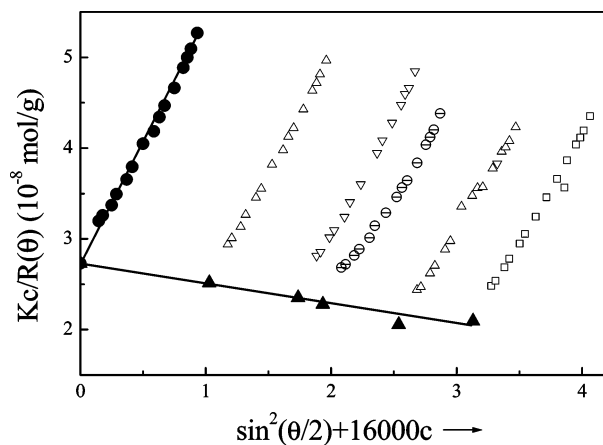


**Figure 7.** Zimm plots of polymerized vesicles prepared from aqueous surfactant mixtures of [MUTB]/[MUBS] = 7:3 with a total concentration of 27 mM. A series of dilute polymerized vesicle solutions (concentrations ranging from  $6.490 \times 10^{-5}$  to  $2.531 \times 10^{-4}$  g/mL) were used for the SLS measurements.

For vesicles formed at a composition of [MUTB]/[MUBS] = 4:6 (total concentration of 27 mM), QLS revealed apparent hydrodynamic diameters of 83 and 87 nm for vesicles before and after polymerization, respectively.

Because the structure of the polymerized vesicles is fixed, it is possible to use SLS to calculate the molar mass and the radius of gyration of the polymerized vesicles. SLS from the polymerized vesicles (Figure 7) yielded a weight-average vesicle molar mass of approximately  $3.7 \times 10^7$  g mol<sup>-1</sup>. This value corresponds to approximately  $6.5 \times 10^4$  MUTB molecules and  $2.8 \times 10^4$  MUBS molecules in each polymerized vesicle, based on the assumption that all the surfactant molecules have participated in the vesicle formation and that the molar ratio of MUTB and MUBS in the polymerized vesicles is the same as the initial ratio, which should be a good assumption for samples at this concentration. The  $z$ -average hydrodynamic radius of gyration ( $\langle R_g \rangle$ ) of the polymerized vesicles is 49.4 nm, and  $\langle R_g \rangle / \langle R_h \rangle = 0.998$ , which is essentially the theoretical value of 1.0 for non-draining thin-layer hollow spheres. These measurements confirm that the vesicle structures have been successfully preserved by polymerization.

**SANS Results.** The SANS spectrum for an unpolymersed vesicle sample composed of MUTB/MUBS = 7:3 (total concentration of 27 mM) is shown in Figure 8 (open triangles). The scattered intensity of the spectrum displays a  $q^{-2}$  dependence, which is a signature of scattering from bilayers and membranes. The spectra are thus qualitatively consistent with the presence of vesicles in solution. Fitting the scattering data to a polydisperse core-shell model yielded a core diameter of  $39.0 \pm 1.8$  nm, a shell (bilayer) thickness of  $3.3 \pm 0.1$  nm, and a polydispersity of  $0.40 \pm 0.03$ . Note that the vesicle diameter obtained by QLS is much larger than that determined by SANS. This is because the vesicle size obtained by QLS is an intensity-averaged value, which is approximately the ratio of the fourth and third moments of the vesicle size distribution  $P(r)$ , that is,<sup>47</sup>

$$\bar{d}_{\text{DLS}} = 2 \left\langle \frac{1}{R} \right\rangle^{-1} = 2 \frac{\int_0^\infty P(r) R^4 dr}{\int_0^\infty P(r) R^3 dr} \quad (1)$$

Hence, for polydisperse samples, the average size obtained using QLS would be significantly higher than

(47) Coldren, B.; van Zanten, R.; Mackel, M. J.; Zasadzinski, J. A. *Langmuir* **2003**, *19*, 5632–5639.

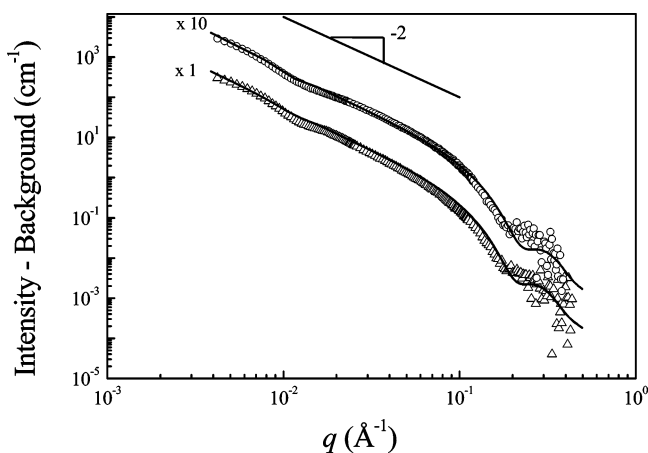


**Figure 8.** SANS data,  $I$ -Background vs  $q$ , for the unpolymerized vesicles (open triangles) and polymerized vesicles (open circles) in  $D_2O$ . The molar ratio of MUTB to MUBS is 7:3 with a total concentration of 27 mM. A polydisperse core-shell model with three adjustable parameters is used to fit both spectra (solid lines). The unpolymerized vesicle core diameter ( $39.0 \pm 1.8$  nm), shell thickness ( $3.3 \pm 0.1$  nm), and polydispersity ( $0.40 \pm 0.03$ ) and the polymerized vesicle core diameter ( $42.4 \pm 3.8$  nm), shell thickness ( $2.9 \pm 0.1$  nm), and polydispersity ( $0.45 \pm 0.07$ ) were obtained by minimizing  $\chi^2$  for the two spectra. For clarity, the scattering curve of the polymerized vesicle sample is shifted by a factor of 10.

the number-averaged size measured using cryo-TEM or SANS. Further, in QLS measurements a small concentration of larger particles or nonspherical microstructures can substantially distort the average hydrodynamic size toward larger values.

For purpose of comparison, the Schulz distribution and the mean core radius, shell thickness, and polydispersity values from SANS were used to evaluate eq 1. The calculation gives a  $z$ -averaged vesicle diameter of 68 nm, which is smaller than the size obtained by QLS (98 nm).

SANS was then used to characterize the polymerized vesicles in  $D_2O$  (Figure 8, open circles). The scattering from this sample also shows a  $q^{-2}$  dependence and essentially overlaps that of the original unpolymerized vesicles. The volume fraction of the original vesicles is about 2.5%, so there is some possibility of intervesicular cross-linking during polymerization. However, SANS results show that there is not appreciable intervesicular cross-linking because of the overlap of the two SANS spectra in the low  $q$  range. This is perhaps expected as all the surfactant monomers are used to form the vesicle structures in the original unpolymerized vesicles and the double bonds are buried inside the hydrophobic bilayers. Therefore, the locus of polymerization is only inside the hydrophobic vesicular shell. Fitting the spectrum from the polymerized vesicles to the core-shell model yields a core diameter of  $42.4 \pm 3.8$  nm, a shell (bilayer) thickness of  $2.9 \pm 0.1$  nm, and a polydispersity of  $0.45 \pm 0.07$ . The  $z$ -averaged vesicle diameter calculated from eq 1 is 77 nm, which is smaller than that obtained from QLS (100 nm).

The shell thickness reduction from  $3.3 \pm 0.1$  to  $2.9 \pm 0.1$  nm (a 12% decrease) after polymerization corresponds to a contraction of the vesicle shell due to volume changes in the bilayers during polymerization. Likewise, the small size increase from  $39.0 \pm 1.8$  to  $42.4 \pm 3.8$  nm for the vesicles after polymerization is within the error bounds of the model and may be the result of partial vesicle fusion

as suggested by the presence of a few irregularly shaped vesicles in the cryo-TEM micrographs (Figure 5). In SANS results, the presence of these morphologies is reflected in a slight increase of  $\chi^2$  for the fit of the SANS data for the vesicles after polymerization. Nevertheless, as seen in Figure 8, the fit for the polymerized vesicles is still very good for all  $q$  values. Thus, SANS data from the original and polymerized vesicles confirm that polymerization has successfully locked in the vesicular structure and the bilayer structure arrangement is preserved. There is no appreciable intervesicle cross-linking, although vesicle fusion may occur to some degree. These results also suggest the fragments and fused vesicles observed by cryo-TEM are relatively scarce.

The SANS data can also be used to calculate the headgroup area ( $a_0$ ) per molecule and the vesicle weight-average molar mass ( $\langle M \rangle_w$ ), the latter of which should correspond to the value directly measured by SLS. Starting from the vesicle excluded volume fraction ( $\phi$ ), core radius, bilayer thickness, and total number of surfactant molecules ( $n_s$ ), the vesicle aggregation number ( $N$ ) and average vesicle area ( $A_v$ ) can be calculated from the expressions

$$N = \frac{n_s \int \frac{4\pi}{3} r^3 P(r) dr}{\phi} \quad (2)$$

$$A_v = \int 4\pi r^2 P(r) dr \quad (3)$$

where  $A_v$  is evaluated separately for the inner and outer surface of the vesicle. Thus,  $a_0$  is obtained from  $a_0 = A_v/N$ . Likewise, the expression for  $\langle M \rangle_w$  has the form

$$\langle M \rangle_w = \frac{\int MW^2(r) P(r) dr}{\int MW(r) P(r) dr} \quad (4)$$

where  $MW(r)$  depends on area per vesicle [ $A = 4\pi(r_{\text{core}}^2 + r_{\text{ext}}^2)$ ], the headgroup area ( $a_0$ ), and the molecular weight and molar ratio of the surfactants. For the vesicles before polymerization,  $a_0$  and  $\langle M \rangle_w$  are calculated to be  $0.28 \text{ nm}^2$  and  $3.13 \times 10^7 \text{ g mol}^{-1}$ , respectively. After polymerization,  $a_0$  and  $\langle M \rangle_w$  are  $0.37 \text{ nm}^2$  and  $3.10 \times 10^7 \text{ g mol}^{-1}$ . The  $a_0$  values before and after polymerization are close to the typical headgroup areas in lamellar phases (ca.  $0.3$ – $0.4 \text{ nm}^2$ ).<sup>48</sup> Perhaps the larger value of  $a_0$  after polymerization reflects the more rigid structure of the fixed bilayer. The  $\langle M \rangle_w$  of the polymerized vesicles determined from SANS is also quite comparable to the weight-averaged vesicle molar mass ( $3.66 \times 10^7 \text{ g mol}^{-1}$ ) determined from SLS for the polymerized vesicles.

## Conclusions

In summary, two polymerizable surfactants, methacryloyloxyundecyl trimethylammonium bromide (MUTB) and sodium 4-( $\omega$ -methacryloyloxyundecyl)oxy benzene sulfonate (MUBS), were synthesized. Vesicles form in mixtures of MUTB and MUBS and can be polymerized. Quasi-elastic and static light scattering, small-angle neutron scattering, and cryo-TEM all show that the vesicle structures have been successfully fixed by polymerization. There is no appreciable intervesicle cross-linking. The size and polydispersity of the original vesicles and polymerized

(48) Nagarajan, R. *Langmuir* **2002**, *18*, 31–38. Bergström, M. *Langmuir* **1996**, *12*, 2454–2463.

vesicles are comparable, as evidenced from light scattering, SANS, and cryo-TEM.

**Acknowledgment.** We acknowledge the support of the National Science Foundation CTS-9814399. The

National Institute of Standards and Technology, Gaithersburg, MD, U.S. Department of Commerce, provided neutron scattering facilities used in this work.

LA035409R